PROCEEDINGS, 43rd Workshop on Geothermal Reservoir Engineering
Stanford University, Stanford, California, February 12-14, 2018
SGP-TR-213

Modified Sequential Fully Implicit Method for Geothermal Reservoir Simulation

Zhi Yang WONG, Ruslan RIN, Hamdi TCHELEPI and Roland HORNE

Department of Energy Resources Engineering, Stanford University, Stanford, CA 94305

zhiyangw@stanford.edu

Keywords: modified sequential, fully implicit, nonlinear formulation, geothermal reservoir simulation

ABSTRACT

This study presents a new sequential coupling strategy for geothermal reservoir simulation – modified sequential implicit (m-SFI) method. The m-SFI method was implemented and tested using the new GENeral Implicit Coupling framework (GENIC) within the Automatic-Differentiation General Purpose Research Simulator (AD-GPRS). This framework allows for the rapid prototyping and consistent testing for this new m-SFI method. In this work, we demonstrated how the m-SFI method performs for several challenging examples where a standard sequential formulation fails. In particular, we showed that for complex flow regimes, the m-SFI method takes a similar number of time steps as the fully implicit method (FIM). It was found that for cases where accurate front prediction is possible and the two-phase region is limited, such as strictly injection or production problems, the m-SFI approach outperforms FIM. However, for a reservoir with mostly two-phases, the overall performance of the m-SFI method is more expensive than FIM due to the increased cost of the sequential iterations.

1. INTRODUCTION

Geothermal simulation plays a crucial part in the management and development of a geothermal field (O'Sullivan et al., 2001). The nonlinearities arising from the multiphase fluid modeling and complexities from the geology result in significant numerical convergence issues (Magnusdottir 2013, Noy et al. 2012). This problem of numerical convergence is intensified in inverse modeling and uncertainty quantification where an ensemble of simulations are run, thus there is a need for fast and robust convergent simulations.

One of the key difficulties for the numerical convergence in geothermal simulations is due to the tight coupling between the mass and energy conservation equations originating from the complex thermodynamic relationships that govern the fluid properties. Additionally, phase change can occur frequently resulting in sharp discontinuities in fluid property calculations. To address this strong coupling, a common approach (Pruess et al., 1999, Zaydullin et al., 2014) is to use a fully coupled and fully implicit method (FIM). Although the FIM ensures numerical stability in the problem, it does not guarantee nonlinear convergence. In addition, both of these conservation equations have parabolic and hyperbolic behavior. The system of equations is parabolic in the flow and conduction and hyperbolic in the transport of mass and energy. Coupling the different physics and flow mechanisms makes it difficult to investigate this nonlinear problem. A separation of the flow and thermal equations could reduce the severity of the nonlinear coupling difficulties and improve understanding of the problem. Depending on the coupling strength of the problem, separating these equations could also reduce the overall computational time, because this reduces the number of linear equations solved. However, problem decoupling could also increase the number of iterations when the coupling is too strong. This result was shown in the geomechanics problem where a fixed-stress sequential coupling could often outperform a fully coupled strategy (Kim et al., 2009, Rin, 2017) for problems with weak coupling between flow and mechanics.

Wong et al. (2017) investigated a sequential splitting of the flow and thermal equations and compared different coupling variable formulations in a sequential strategy. They found that a naive constant pressure approach performed the best for single-phase blocks and a constant density approach performed best for two-phase blocks. From this, a hybrid approach was proposed where constant pressure was used for single-phase blocks and a constant density was used for two-phase blocks. This hybrid approach performed the best out of all the sequential strategies that were investigated. However, it was shown that for more challenging problems the fully coupled fully implicit method performs significantly better than any of the sequential schemes implemented.

This work aimed to build upon the findings in Wong et al. (2017) to develop a modified sequential method that can overcome the poor convergence in the previously described sequential strategies. Specifically, this work proposed a modified sequential fully implicit method (m-SFI) method for geothermal simulations. This m-SFI method was inspired by a similar m-SFI method (Moncorge et al. 2017) proposed for compositional flow simulations. In Moncorge et al. (2017), their scheme involved enriching the 'standard' pressure equations with coupling between the pressure and saturation/compositional variables for the blocks that had a strong coupling between flow and transport. Their criterion for defining strongly coupled blocks was blocks that had flow transfer between different fluid phases in the block and their neighboring cells. A similar intuition of including the strongly coupled blocks was used for the proposed m-SFI formulation that is described in later sections.

2. NUMERICAL FORMULATION

2.1 Governing Equations

For this study, only the flow and thermal equations of pure water in two-phase flow was considered. The flow and thermal equations are the mass and thermal conservation equations:

$$F = \frac{\partial}{\partial t}\left(\phi(\rho_w S_w + \rho_s S_s)\right) - \nabla.(\rho_w u_w + \rho_s u_s) - Q_M = 0 \tag{1}$$

and

$$\begin{aligned} T = \frac{\partial}{\partial t}\left((1-\phi)\rho_R U_R + \phi(\rho_w U_w S_w + \rho_s U_s S_s)\right) \\ - \nabla.(\rho_w h_s u_w + \rho_s h_s u_s) - \nabla.(K\nabla T) - Q_E \\ = 0 \end{aligned} \tag{2}$$

where:

- ϕ is the porosity of the rock
- ρ_k is the mass density of phase k
- S_k is the saturation of phase k
- u_k is the velocity of phase k
- Q is the source/sink term
- h_k is the enthalpy of phase k
- U_k is the internal energy of phase k
- K is the total conductivity of the fluid and rock

Here the subscripts w/s represent the two phases water and steam, and the subscript R represents the rock. Both ρ_k, h_k in each phase depend on the phase state of the fluid. The thermodynamic parameters that were used for this study had all the parameters as a function of p and h of the block (Faust and Mercer, 1979).

In addition to these two conservation equations, the saturation constraint must be satisfied, the sum of all the phase saturations is equal to one.

$$S_w + S_s = 1 \tag{3}$$

2.2 Darcy's Law

To model the velocity of each phase, Darcy's law was used to describe the flow through the porous media:

$$u_k = -\frac{k k_{rk}}{\mu_k}\nabla(p_k + \rho_k g z) \tag{4}$$

where:

- u_k is the superficial velocity of phase k
- k is the rock permeability
- k_{rk} is the relative permeability of phase k
- μ_k is the viscosity of phase k
- p_k is the pressure of phase k
- g is the gravitational constant
- z is the direction of the gravity
- k represents either the water phase or steam phase

The two-point flux approximation (TPFA) finite volume method and a fully implicit method was implemented to discretize the flow and thermal conservation equations (Equations 1 and 2) in space and time. The analysis for this entire study will use the phase-based, single point upstream weighted TPFA scheme.

2.2 Fully Coupled Formulation

The finite volume approximation results in the system of nonlinear equations for flow and thermal energy.

$$\begin{aligned} R_F^{n+1}(x_F^{n+1}, x_T^{n+1}) = \ & \left(\phi(\rho_w S_w + \rho_s S_s)\right)^{n+1} - \left(\phi(\rho_w S_w + \rho_s S_s)\right)^{n} \\ & - \nabla.(\rho_w u_w + \rho_s u_s)^{n+1} - Q_M^{n+1} = 0 \end{aligned} \tag{5}$$

and

$$
\begin{aligned}
R_T^{n+1}(x_F^{n+1}, x_T^{n+1}) = {} & \left((1-\phi)\rho_R U_R + \phi(\rho_w U_w S_w + \rho_s U_s S_s)\right)^{n+1} \\
& - \left((1-\phi)\rho_R U_R + \phi(\rho_w U_w S_w + \rho_s U_s S_s)\right)^{n} \\
& - \nabla.(\rho_w h_s u_w + \rho_s h_s u_s)^{n+1} - \nabla.(K\nabla T)^{n+1} \\
& - Q_E^{n+1} = 0
\end{aligned} \tag{6}
$$

Here the variables x_F^{n+1}, x_T^{n+1} represents the primary variables for the flow and thermal equations at the time level $(n+1)$. The typical fully implicit (FIM) involves solving all the residual equations simultaneously.

$$
\begin{aligned}
R_F^{n+1}(x_F^{n+1}, x_T^{n+1}) = 0 \\
R_T^{n+1}(x_F^{n+1}, x_T^{n+1}) = 0
\end{aligned} \tag{7}
$$

Using Newton's method to solve this system of nonlinear equations this leads to:

$$
\begin{bmatrix}
\frac{\partial R_F}{\partial x_F} & \frac{\partial R_F}{\partial x_T} \\
\frac{\partial R_T}{\partial x_F} & \frac{\partial R_T}{\partial x_T}
\end{bmatrix}
\begin{bmatrix} \delta x_F \\ \delta x_T \end{bmatrix} = -\begin{bmatrix} R_F \\ R_T \end{bmatrix} \tag{8}
$$

Here we used pressure and total enthalpy ($x_F \coloneqq p, x_T \coloneqq h$) as the primary variables (Wong et al., 2016).

2.3 Modified Sequential Fully Implicit Formulation

For the modified sequential fully implicit formulation (m-SFI), the flow and thermal equations are solved separately for their respective primary variables x_F, x_T. The main difference between the modified sequential fully implicit method and the standard sequential implicit method is that in the first step where flow is solved, a subset of the thermal equations are included in this step. For this study, we only examined a sequential formulation for a pressure-enthalpy formulation as described in Wong et al. (2016), although a sequential formulation for using natural variables (Coats, 1980) is possible. The pressure-enthalpy formulation was selected as it does not require any variable switching and thus allows for a simpler implementation and analysis for this method. It is important to note that this sequential formulation is iteratively coupled until convergence is reached for both the flow and thermal equation. The steps for the m-SFI are as follows:

Step 1: Solve:

$$
\begin{aligned}
R_F^{n+1}(x_F^{n+1}, x_T^{n+1}) = 0 \\
R_T^{n+1}(x_F^{n+1}, x_T^{n+1}) = 0
\end{aligned} \tag{9}
$$

for blocks in M_1, and:

$$
R_F^{n+1}(x_F^{n+1}, x_T^{n+1}(\delta h^{n+1} = 0)) = 0 \tag{10}
$$

for the remaining blocks not in M_1.

This involves solving the flow equation with a variable $\delta h = 0$ for those blocks that are not in the domain M_1, the choice of this variable does affect the convergence, but because all of these blocks are at single-phase, a constant enthalpy was chosen. Once we have the solution, we use that as the initial guess to the solution of the thermal equation.

Step 2: Solve:

$$
R_T^{n+1}(x_F(\delta p = 0), x_T^{n+1}) = 0 \tag{11}
$$

for blocks in M_2

This involves solving the thermal residual equations for the blocks in M_2 while assuming $\delta p = 0$ for those blocks. The choice of M_1 and M_2 is the focus of this work. In both steps we are solving a system of nonlinear equations which is solved using Newton's method. These two steps (Equation 9) and 2 (Equation 10) are repeated sequentially until convergence.

2.3.1 Subdomain definition

We define M_1 as the subdomain that has strong coupling between the flow and thermal equations and M_2 is the weakly coupled domain. In this work we investigated different definitions of these strongly coupled and weakly coupled domains. We measured the strength of the coupling based on the Courant-Friedrichs-Lewy (CFL) of the block and the phase state of the block.

$$
\mathrm{CFL} = \frac{\Delta t Q}{PV} \tag{12}
$$

where:

- Δt is the maximum time step
- Q is the volume injection rate
- PV is the pore volume of the block

We define a block i to be in M_1 if any of the below conditions are satisfied:

- $\mathrm{CFL_i} > \mathrm{CFL_{tol}}$ OR Number Phases of block i > 1 OR A well perforation penetrates block i

We also investigated adding all the neighboring blocks that satisfy the above criterion. This was to limit the discontinuities between the flow and thermal steps. We refer to this strategy as m-SFI-N.

The criterion for M_2 is the complement of M_1:

- $\mathrm{CFL_i} < \mathrm{CFL_{tol}}$ AND Number Phases of block $i == 1$ AND no well perforation penetrates block i

3. IMPLEMENTATION

3.1 AD-GPRS

The implementation and comparisons for this study was completed using AD-GPRS. AD-GPRS was designed to have a general sequential-implicit coupling framework for solving multiphysics problems for reservoir simulation (Rin et al., 2017). This framework allows the consistent testing and development of different sequential implicit for different coupling strategies to obtain robust and scalable multiphysics problems such as geothermal simulations (Wong et al., 2015, Wong et al., 2016). This work exploited the integration of the geothermal module in AD-GPRS to the next generation general sequential framework in AD-GPRS and tested the m-SFI methods utilizing the sequential framework (Rin et al., 2017). The framework employed a modular design by splitting the flow and thermal conservation equations into a set of two subproblems. The key components of this framework involve using a subproblem tree structure with abstract computational domains to organize the unknowns related to each subproblem. This flexible framework is the core of the investigation the m-SFI method. This both allows for minimal code duplication but also provides a consistent framework for the comparisons.

One of the key flexibilities of the framework is the inclusion of mapping operators. In GENIC, a mapping operator specifies the active domain that can change dynamically with each Newton iteration. This mapping operator allows for the flexibility in testing different criteria and definitions for the M_1 and M_2 subdomains.

In addition to the general implicit coupling framework, Automatic-Differentiation General Purpose Research Simulator (AD-GPRS) (Voskov and Tchelepi, 2012, Zhou, 2012) has a wide range of capabilities in advanced physical modeling and numerical methods. These capabilities include thermal-compositional, EOS-based, multiphase flow and transport models (Zaydullin et al., 2014; Voskov et al., 2016), generalized nonlinear formulations (Voskov, 2012, Zaydullin et al., 2013), multistage linear solvers (Zhou et al., 2013, Klevtsov et al., 2016), complex multisegment wells (Zhou, 2012), and nonlinear mechanical deformation models (Garipov et al., 2015, 2016).

4. NUMERICAL COMPARISONS

Here we considered two three-dimensional problems that each have the characteristics of a challenging geothermal model. The first problem has three-dimensional and strong two-phase gravitational effects and the second is a three-dimensional problem with strong geological heterogeneity. The verification of the fully implicit and sequential implicit results was done in Wong et al. (2017) where the fully implicit, sequential results were compared with analytical, semianalytical and TOUGH2 simulations. Here the focus will be to compare the convergence properties of m-SFI method with the fully implicit solution.

To decouple the effects of the linear solver solution on the nonlinear solver, a direct solver PARDISO (Petra et al., 2014a, Petra et al., 2014b, Schenk and Gärtner, 2004) was used for the linear solver. In all the cases, the maximum sequential iterations was set to be 30, the maximum nonlinear iterations was set to 20, and the convergence tolerance for the flow and thermal equations was set to 10^{-4}. However, the use of a direct solver limits any strong conclusions on the computational speed up.

4.1 3D Two-phase Gravity Drainage Problem

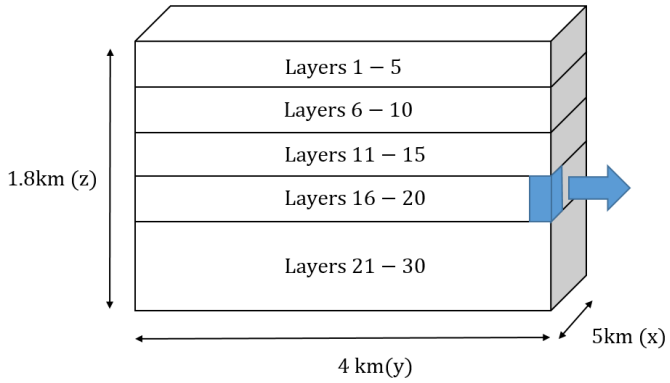

Figure 1: Schematic of the three-dimensional two-phase gravity drainage model

4.1.1 Model Description and Verification

The first test case is a three-dimensional model based on a reservoir model from the 1980 Code Comparison Study (Stanford Geothermal Program, 1980). This reservoir model consists of single-phase liquid water with a two-phase zone of immobile steam wedged between a cold and hot water region. Fluid is produced from a single well that is completed below the two-phase zone. The rock and reservoir properties (Table 1) were selected such that the boiling in the well occurs after a certain period of production. The parameters for this study are relatively homogeneous but due to the complex fluid behavior that is typical of geothermal fields it is suitable as a test case. A full discussion on the problem description can be found in Stanford Geothermal Program (1980). The production well was completed in the corner block and perforates layers 16-20. Water was produced at a rate of 500m^3/day for 10 years. Figure 1 shows a schematic of the well and the reservoir.

Table 1: Reservoir properties for the 3D Two-phase Gravity Drainage Problem

Reservoir dimensions (m)	$4000 \times 5000 \times 1800$
Porosity in each layer	[0.2,0.25,0.25,0.25,0.2,0.2]
Layer permeability in x and y directions (md)	[100,200,200,200,100,100]
Layer permeability in z direction	[2,50,50,50,2,2]
Layer gas saturation	[0,0.15,0,0,0,0]
Depth at layer top (m)	[150,450,750,1050,1350,1650]
Temperature at layer top (K)	[433.15,553.15, …,553.15]
Pressure at layer top (bar)	[40,64,88,112,136,160]

The final pressure and temperature distributions are shown in Figure 2. The relative difference between the pressure and temperature for FIM and m-SFI is shown in Figure 3. We can see that there is very close agreement where the difference is at most 0.01%. This is expected since the FIM and m-SFI method both require the flow and thermal residual equations to be below a convergence tolerance, thus if converged they should have close agreement.

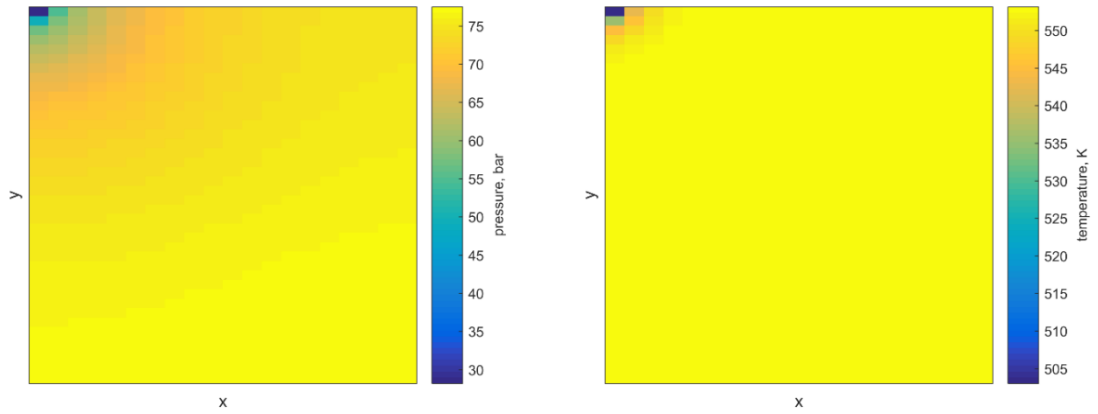

Figure 2: 3D Pressure and temperature distribution after 10 years of production at 16th layer for 20× 40 × 36 blocks

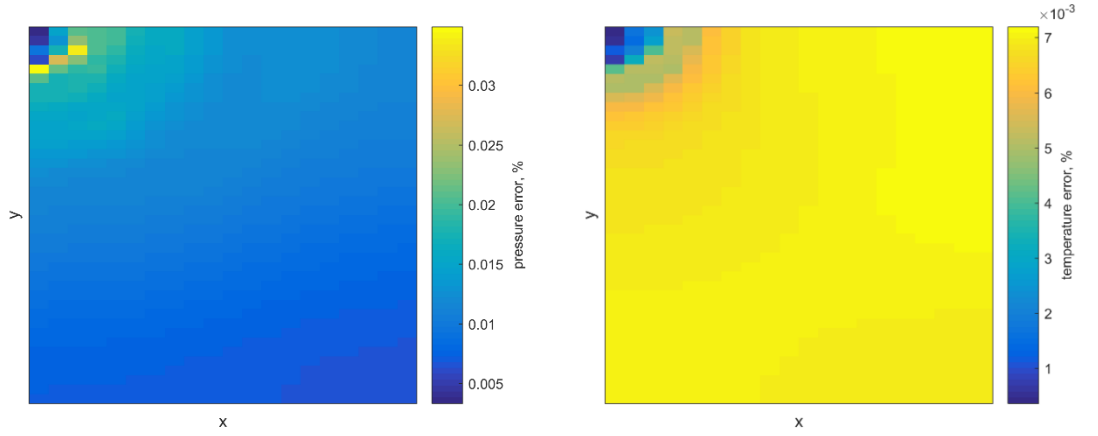

Figure 3: Relative error between FIM and m-SFI-N approach for pressure and temperature after 10 years at 16th layer for 20× 40 × 36 blocks

4.1.2 Nonlinear Convergence Comparison

The focus of this section is to compare the performance of the m-SFI method with FIM for this test case. Table 2 shows the nonlinear solver performance for the different strategies tested. We see that for this specific test case, regardless of the $\mathbf{CFL_{tol}}$ selected, the m-SFI methods converge to the same maximum CFL (maximum CFL is defined as the maximum CFL for all the blocks for all the time steps) as the FIM and has less wasted time steps than the FIM. We also see that the m-SFI method is able to overcome the limitations that the sequential strategy had for complex problems and decreased the number of sequential iterations per timestep by 10 times. For this specific case, a $\mathbf{CFL_{tol}}$ of [0.1,1,10] all resulted in about the same performance. This is because at this grid resolution, the complexity is not sufficient to demonstrate the effects of different $\mathbf{CFL_{tol}}$ values or the inclusion of neighboring blocks.

Table 2: Comparison of the nonlinear solver performance for the different coupling schemes for 10×20×18 blocks

			m-SFI			
	FIM	**SEQ**	$\mathbf{CFL_{tol} = 0.1}$	$\mathbf{CFL_{tol} = 1}$	$\mathbf{CFL_{tol} = 10}$	**m-SFI-N**
Number of timesteps	40	215	39	39	39	39
Total Newton Iterations	136	5050	306	308	324	213
Total sequential iterations	0	6681	134	136	137	105
Sequential iterations/timesteps	-	31.1	3.4	3.5	3.5	2.7
Number of timesteps wasted	4	201	1	1	1	1
% of blocks in M_1	100	0	27.89	19.25	19.06	30.30
Maximum CFL	5.343	2.707	5.342	5.342	5.342	5.342

The original grid was coarsened and refined to test how the m-SFI method performs with different $\mathrm{CFL_{tol}}$. Here we looked at a low resolution ($4 \times 5 \times 6$ blocks) and a high resolution ($20 \times 40 \times 36$ blocks) grid. Table 3 shows the results of the different resolutions for the different methods. For the low resolution, we see that similar to the previous case, the m-SFI methods all have the same time stepping result and converge for the same maximum CFL. However for the refined case (H), only the m-SFI-N method has the same time stepping result as the fully coupled method. We notice that regardless of the $\mathrm{CFL_{tol}}$ selected, the number of time steps is still higher than the fully coupled and m-SFI-N method. We see that now as there more phase change and there is a sharper boundary to the two-phase region, having the additional layer of neighboring cells significantly increases the convergence properties. We note that at the high resolution, the m-SFI-N method performs 10% faster than the fully coupled method. This computational speed up is a combination of the relatively low number of sequential iterations per time step and small % of blocks in M_1. As mentioned earlier, since only a direct linear solver is used, it is difficult to conclude that the m-SFI-N can indeed outperform FIM.

Table 3: Comparison of the nonlinear solver performance for two-phase gravity drainage problem at different grid resolutions (L: Low, H: High)

			m-SFI							
	FIM		$\mathbf{CFL_{tol} = 0.1}$		$\mathbf{CFL_{tol} = 1}$		$\mathbf{CFL_{tol} = 10}$		**m-SFI-N**	
Grid resolution	**L**	**H**	**L**	**H**	**L**	**H**	**L**	**H**	**L**	**H**
Number of timesteps	19	162	19	584	19	592	19	592	19	162
Total Newton Iterations	28	454	67	1982	67	2004	67	2016	41	585
Total Sequential Iterations	-	-	49	1901	49	1918	49	1946	40	470
Sequential iterations/timesteps	2.6	3.3	2.6	3.2	2.6	3.3	2.1	2.9	2.6	3.3
Number of time steps wasted	0	1	0	433	0	436	0	436	0	1
% of blocks in M_1	100	100	19.9	16.8	17.5	15.8	17.5	15.2	50.8	24.4
Maximum CFL	0.51	4.07	0.51	4.0	0.51	4.07	0.5	4.07	0.51	4.07

4.2 SPE 10 Three-dimensional Problem

4.2.1 Model Description and Verification

The permeability and porosity distribution (Figure 5) were taken from the top four layers of the SPE 10 test case problem (Christie and Blunt 2001), Table 4 shows the reservoir properties for this SPE10 problem. For this test case, the domain was discretized using $60 \times 220 \times 4$ blocks. Uniform pressure (50 bar), temperature (523.26 K) and water saturation (1.0) was imposed as the initial conditions. There were four wells specified in this problem, two injectors (P = 90 bar, T = 433.15K) and two producers (P = 30 bar) all operating

under bottom hole pressure control. This problem is highly heterogeneous and follows a Gaussian distribution with high contrast and channelized rock structure. Due to this heterogeneity, this is challenging even for the fully coupled methods and has convergence issues for more aggressive time step schemes. The final pressure and temperature solution for the simulated period is presented in Figure 5.

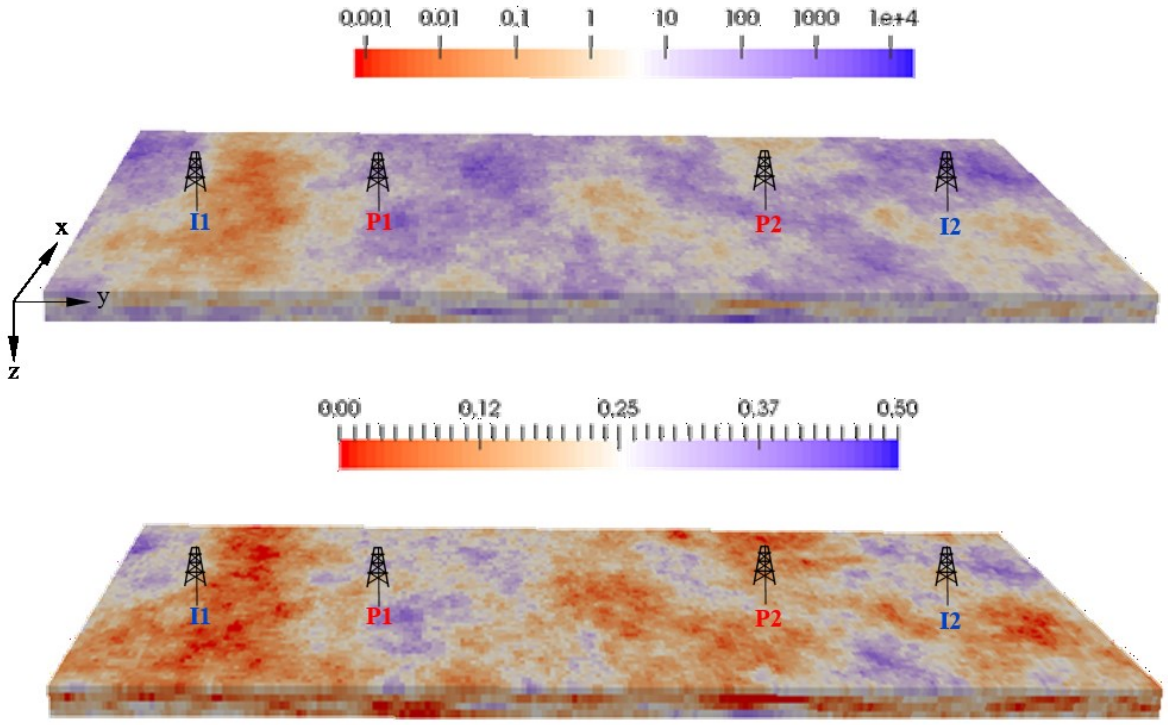

Figure 4: Schematic of SPE 10 problem: Permeability (Top) and Porosity (Bottom)

Table 4: Reservoir properties for 3D SPE 10 Problem

Reservoir dimensions (m)	365.8×670.6× 51.8
Initial reservoir pressure (bar)	50
Initial reservoir (K)	523.26
BHP (bar)	30 for producers, 90 for injectors
Injection temperature (K)	433.15
Relative phase permeability	$k_{rj} = S_j^2$
Rock thermal expansion (1/K)	2×10^{-5}
Rock heat capacity (kJ/(kg K))	2000.0
Rock thermal conductivity (kJ/(m day K))	150.0
Water thermal conductivity (kJ/(m day K))	53.5
Gas thermal conductivity (kJ/(m day K))	3.59

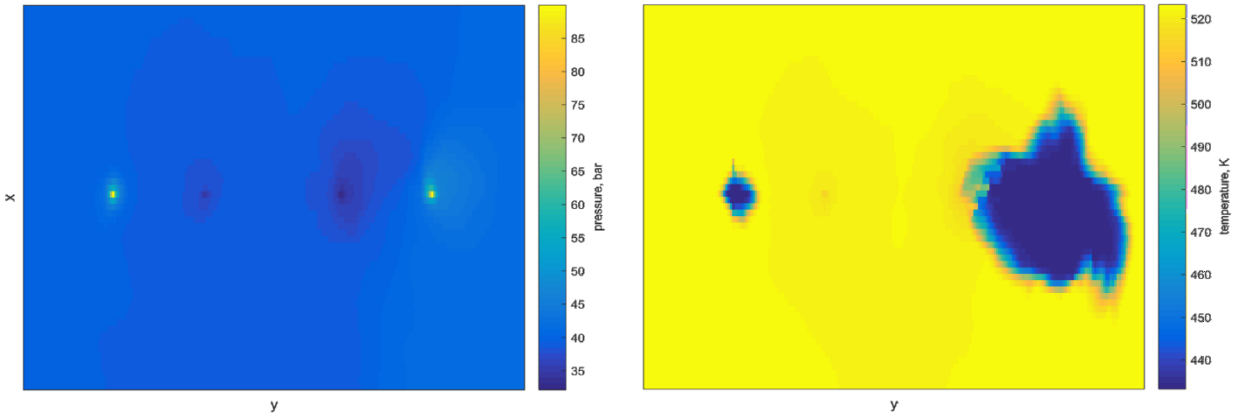

Figure 5: Pressure (left) and temperature (right) distribution for 60 220 4 grid after 100 days at top layer

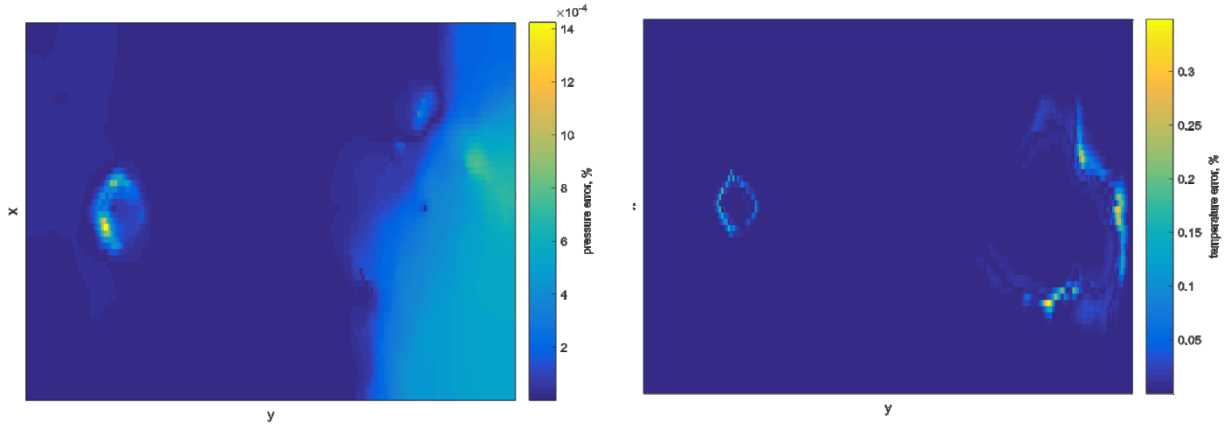

Figure 6: Relative difference between FIM and m-SFI-N approach for pressure (left) and temperature (right) distribution for 60×220×4 grid after 100 days at top layer

We see in Figure 6, the relative difference between the FIM and m-SFI-N method is slightly higher than the previous two-phase gravity drainage problem. For this specific scenario, the error is 10^{-3}% for pressure and at most 0.5% for the temperature. This error is localized at the temperature front.

4.2.2 Nonlinear Convergence Comparison

Table 5 shows the results of the different methods for a grid structure of $30 \times 110 \times 2$ blocks. Here we notice that the m-SFI-N at a CFL_{tol} of 0.1 requires about half the number of time steps in comparison to a CFL_{tol} of 1. This is because with a smaller CFL, this means we have a larger number of blocks in each iteration thus are able to capture the front better. We see that the percentage of blocks is more for the case where $CFL_{tol} = 1$; this is because of the number of time step cuts and thus more iterations are spent where the front has spread. Due to the injection and production fronts in this problem, we notice that m-SFI ($CFL_{tol} = 0.1$) performs better than m-SFI-N ($CFL_{tol} = 1$) due to the need to predict where the front is accurately.

Table 5: Comparison of the nonlinear solver performance for the different coupling schemes for 30×110×2 blocks

	FIM	m-SFI ($\mathbf{CFL_{tol} = 0.1}$)	m-SFI-N ($\mathbf{CFL_{tol} = 1}$)	m-SFI-N ($\mathbf{CFL_{tol} = 0.1}$)
Number of timesteps	53	75	111	53
Total Newton iterations	179	1869	3974	793
Total sequential iterations	-	797	1599	377
Sequential iterations/timesteps	-	10.6	14.4	7.1
Number of timesteps wasted	9	37	81	8`
% of blocks in M_1	100	71.75	74.81	67.42
Normalized Run time	1	8.3	17.43	3.15
Maximum CFL	44.13	44.24	42.04	44.18

Table 6 shows the results for a low $(15 \times 55 \times 1)$ and high $(60 \times 220 \times 4)$ grid resolution. In order to coarsen and refine the grid, volume averaged properties were used for the porosity and permeability. Here we see that for a low resolution, all four of the methods result in the same number of timesteps to complete the simulation. For the high grid resolution, only the m-SFI-N method had a comparable maximum CFL and similar number of time steps. However, all the m-SFI cases are four times slower compared to FIM. This is due to the higher number of sequential iterations per time step than in the previous test case and the larger percentage of blocks in the M_1 subdomain, thus having a larger cost per sequential step. In summary, we have found that for this case where there is a large proportion of two-phase blocks, the m-SFI method performs poorly, because most blocks have a strong coupling, there is not much gain in splitting the flow and thermal equations sequentially.

Table 6: Comparison of the nonlinear solver performance for two-phase gravity drainage problem at different grid resolutions (L: Low, H: High)

	FIM		m-SFI ($\mathbf{CFL_{tol} = 0.1}$)		m-SFI ($\mathbf{CFL_{tol} = 1}$)		m-SFI-N ($\mathbf{CFL_{tol} = 0.1}$)	
	L	**H**	**L**	**H**	**L**	**H**	**L**	**H**
Number of timesteps	49	114	49	126	49	177	49	115
Total Newton iterations	77	443	708	4077	1061	8203	708	3412
Total Sequential Iterations	-	-	371	1509	476	2969	371	1323
Sequential iterations/timesteps	-	-	7.6	12.0	9.7	16.8	7.6	11.5
Number of timesteps wasted	0	19	0	40	0	106	0	21
% of Blocks in M_1	100	100	55.18	70.62	22.13	68.6	55.2	74.2
Normalized run time	1	1	4.92	4.83	6.69	10.2	4.91	4.15
Maximum CFL	59.4	62.4	59.4	62.2	59.4	62.7	59.4	62.4

5. CONCLUSIONS

In this study, we investigated a new modified sequential coupling approach for geothermal simulations. We demonstrated the capability of the m-SFI method on two difficult problems where the sequential formulation described in Wong et al. (2017) performed poorly. For these challenging problems, the m-SFI achieved a number of time steps comparable to a fully coupled method. For cases where accurate front prediction is possible and the two-phase region is small, the m-SFI approach outperformed the FIM. However, for cases where the domain is mostly two-phase, the overall performance of the m-SFI is more expensive than the FIM due to the increased sequential iterations per time step and the cost of each sequential step.

REFERENCES

Christie, M. A., & Blunt, M. J. (2001). Tenth SPE comparative solution project: A comparison of upscaling techniques. In SPE Reservoir Simulation Symposium. Society of Petroleum Engineers.

Coats, K. H. (1980). An equation of state compositional model. Society of Petroleum Engineers Journal, 20(05), 363-376.

Faust, C. R. and Mercer, J. W. (1979). Geothermal reservoir simulation: 2. numerical solution techniques for liquid-and vapor-dominated hydrothermal systems. Water Resources Research, 15(1):31–46.

Garipov, T., Voskov, D., and Tchelepi, H. A. (2015). Rigorous coupling of geomechanics and thermal compositional flow for SAGD and ES-SAGD operations. In SPE Canada Heavy Oil Technical Conference. Society of Petroleum Engineers.

Garipov, T. T., White, J., Lapene, A., and Tchelepi, H. A. (2016). Thermo-hydro-mechanical model for source rock thermal maturation. In 50th US Rock Mechanics / Geomechanics Symposium, Houston, USA. Society of Petroleum Engineers.

Kim, J., Tchelepi, H. A., & Juanes, R. (2009). Stability, accuracy and efficiency of sequential methods for coupled flow and geomechanics. In SPE reservoir simulation symposium. Society of Petroleum Engineers.

Klevtsov, S., Castelletto, N., White, J. A., and Tchelepi, H. A. (2016). Block-preconditioned Krylov methods for coupled multiphase reservoir flow and geomechanics. In ECMOR XIV-15th European Conference on the Mathematics of Oil Recovery.

Magnusdottir, L. (2013). Fracture Characterization in Geothermal Reservoirs Using Time-lapse Electric Potential Data. PhD thesis, Stanford University.

Moncorgé, A., Tchelepi, H. A., & Jenny, P. (2017). Modified sequential fully implicit scheme for compositional flow simulation. *Journal of Computational Physics*, *337*, 98-115.

Noy, D., Holloway, S., Chadwick, R., Williams, J., Hannis, S., and Lahann, R. (2012). Modelling large-scale carbon dioxide injection into the bunter sandstone in the UK southern north sea. International Journal of Greenhouse Gas Control, 9:220–233.

Petra, C. G., Schenk, O., & Anitescu, M. (2014a). Real-time stochastic optimization of complex energy systems on high-performance computers. Computing in Science & Engineering, 16(5), 32-42.

Petra, C. G., Schenk, O., Lubin, M., & Gärtner, K. (2014b). An augmented incomplete factorization approach for computing the Schur complement in stochastic optimization. SIAM Journal on Scientific Computing, 36(2), C139-C162.

Pruess, K., Oldenburg, C., and Moridis, G. (1999). Tough2 user's guide version 2. Lawrence Berkeley National Laboratory.

Rin, R. (2017). Implicit Coupling Framework for Multi-physics Reservoir Simulation (Doctoral dissertation, Stanford University)

Rin, R., Tomin, P., Garipov, T., Voskov, D., & Tchelepi, H. (2017). General Implicit Coupling Framework for Multi-Physics Problems. In *SPE Reservoir Simulation Conference*. Society of Petroleum Engineers.

Schenk, O., & Gärtner, K. (2004). Solving unsymmetric sparse systems of linear equations with PARDISO. Future Generation Computer Systems, 20(3), 475-487.

Schenk, O., & Gärtner, K. (2006). On fast factorization pivoting methods for sparse symmetric indefinite systems. Electronic Transactions on Numerical Analysis, 23(1), 158-179.

Wong, Z. Y., Horne, R., & Voskov, D. (2015). A Geothermal Reservoir Simulator in AD-GPRS. In Proceedings World Geothermal Congress 2015.

Wong, Z. Y., Horne, R., & Voskov, D. (2016) Comparison of Nonlinear Formulations for Geothermal Reservoir Simulations. 41st Workshop on Geothermal Reservoir Engineering.

Wong, Z. Y., Rin, R., Tchelpi, H. & Horne, R. (2017) Comparison of a Fully Implicit and Sequential Implicit Formulation for Geothermal Reservoir Simulations. 42nd Workshop on Geothermal Reservoir Engineering.

Voskov, D. V. and Tchelepi, H. A. (2012). Comparison of nonlinear formulations for two-phase multi-component eos based simulation. Journal of Petroleum Science and Engineering, 82:101–111.

Voskov, D., Zhou, Y., and Volkov, O. (2012). Technical description of AD-GPRS. Energy Resources Engineering, Stanford University.

Voskov, D., Zaydullin, R., and Lucia, A. (2016). Heavy oil recovery efficiency using SAGD, SAGD with propane co-injection and STRIP-SAGD. Computers & Chemical Engineering, 88:115–125.

Zaydullin, R., Voskov, D. V., James, S. C., Henley, H., & Lucia, A. (2014). Fully compositional and thermal reservoir simulation. Computers & Chemical Engineering, 63, 51-65.

Zhou, Y., Jiang, Y., and Tchelepi, H. A. (2013). A scalable multistage linear solver for reservoir models with multisegment wells. Computational Geosciences, 17(2):197–216.